Three-Dimensional Analysis of a Through Hole with Radiation Characteristics by the Spatial Network Method

TOHRU ONOJIMA, TATSUYA KASHIWA, MEMBER, IEEE, NORINOBU YOSHIDA, MEMBER, IEEE, AND ICHIRO FUKAI, MEMBER, IEEE

Abstract—**In recent electronic devices, a through hole has been used for mutual connections between layers of printed circuit boards, multilayer wirings on the silicon surface of LSI, and external connections of IC packages. With recent uses of through holes in superminiaturized systems for super-high-frequency waves and ultra-high-speed pulse waves, the influences of the holes not only on the propagation characteristics of the lines but also on the properties of other elements are becoming more pronounced. Therefore to understand the characteristics of the total system, analyses of the electromagnetic field as affected by through holes become indispensable. It is especially necessary to consider the radiation characteristics from a through hole since the radiation affects other lines and devices. However through holes generate complicated distributions of electromagnetic fields owing to their three-dimensional structures. It is necessary to perform rigorous vectorial analyses for three-dimensional fields by using all field components, boundary conditions, and properties of the medium.**

Hence we applied the spatial network method to this analysis. The method has many features for analysis of three-dimensional electromagnetic fields in the time domain. We have already simulated the basic field behavior of the through hole by this method. Such a time-dependent analysis of electromagnetic fields has shown its utility not only in clarifying the variation of the fields in time but also in providing information on the mechanisms by which the distributions of a field at the stationary state are brought about.

In this paper, the radiation characteristics of the through hole are discussed. For the near field, the Poynting vector is important in knowing the field characteristics by the energy flow property. Therefore the variation of Poynting vector distributions near the through hole is simulated in the time domain. Finally, from the distribution of the electric field on the top plane of the through hole that contains the connected stripline and the land, the far-field patterns are computed by the Fourier transform. It is shown that the fundamental characteristics of the radiation from the through hole are thereby obtained.

I. Introduction

OWING TO the remarkable progress recently made in semiconductor technology, the following benefits have been realized: smaller sizes, lighter weights, the ability to perform a multiplicity of functions, higher reliability, and lower costs [1]. In this progress, multilayer wirings in printed circuit boards and in multilayer structures in LSI have served as a basic technology for constructing high-density circuits. In circuits with multiple layers, the use of through holes has become indispensable for connections between layers. Furthermore, external connections of an IC package to the terminal on a printed board may be performed by a through-hole structure. The recent use of through holes in superminiaturized systems for superhigh frequencies and ultra-high-speed pulse waves has given rise to complicated electromagnetic fields by reflection and scattering. These influence not only the propagation characteristics of the line but also the other elements in the circuit. Therefore to understand the characteristics of the system, it is indispensable to analyze the total electromagnetic field as influenced by the through hole. In these influences of the through holes, radiation characteristics are especially important since the radiation affects other lines and devices. As all components of the electromagnetic fields are generated due to the three-dimensional structure of the through hole, vector analysis methods are indispensable [2], [3]. However, a rigorous analysis with complex boundary and medium conditions is difficult. Therefore a numerical analysis is demanded for these problems. Time-dependent analysis of electromagnetic fields has shown its utility not only in clarifying the variation of the fields in time but also in providing information on mechanisms by which the distributions of a field in the stationary state are brought about.

A spatial network method [4] has been proposed for analyzing the time response of electromagnetic fields in three-dimensional fields (referred to here as the present method). We have demonstrated useful results [5]–[7] in many situations by utilizing the features of the present method. In particular we showed that we could easily handle the input conditions, free-space boundary conditions, and the conditions for the medium through its equivalent circuit. Therefore the formulation by the present method is effective for three-dimensional problems such as a through hole. We have applied the method to analyses of through holes and shown the basic properties of it. The frequency responses of reflected and transmitted waves are obtained by applying Fourier transforms to the time-dependent responses of the electric fields for the pulse waves. Through these representations, we showed that it was possible to analyze the three-dimensional field

Manuscript received September 7, 1989; revised January 9, 1990.
The authors are with the Department of Electrical Engineering, Hokkaido University, Sapporo 060, Japan.
IEEE Log Number 9034886.

0018-9480/90/0600-0770$01.00

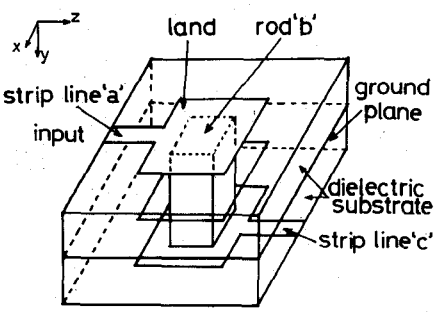

Fig. 1. Analyzed model of a through hole.

and the features of the through hole by the present method [8]–[13].

In this paper, firstly, the electromagnetic field near the through hole obtained by the present method is simulated, and the time responses of the Poynting vector are presented since they are important for knowing the field characteristics by the energy flow. In the present method the near field is calculated only in the finite analyzed region, since the far field must be computed from the near field. Secondly, by applying the Fourier transform to the component of the electric field on the top plane of the through hole that includes the connected stripline and the land, the far-field patterns are obtained. It will be shown that the fundamental characteristics of the radiation from the through hole are thereby obtained.

In Section II, for a simple explanation of the present method in treating the analyzed model of the through hole, we explain the equivalent circuit for the boundary conditions of the through hole at the perfect conductor surface. In Section III, we describe the method for calculating the far-field pattern from the near field. In Section IV, we present the time variation of the Poynting vector in a representative plane. Furthermore we show the components of the electric field in the top plane that contains the connected stripline and the land. By applying the Fourier transform to this electric field distribution, we obtain the far-field pattern and discuss the basic features of radiation characteristics from the through hole.

II. Analytical Model of a Through Hole

A. Analytical Model

Fig. 1 shows a model of a through hole structure which connects the upper and lower striplines through the ground plate. The upper stripline a is connected to the lower stripline c through the ground plate by means of the rod b. The dimensions of the model used are normalized by the spatial interval between nodes Δd (in this analysis, $1\Delta d = 0.125$ mm) and the lengths along the x, y, and z axes are respectively $80\Delta d$, $60\Delta d$, and $90\Delta d$. We placed the ground plate at the midplane parallel to the $x-z$ plane separating the upper and lower layers. There is a square hole (of side $40\Delta d$) for passing the rod. The widths of striplines a and c are $8\Delta d$. The height from the ground plate is $20\Delta d$, which is equal to the thickness of the dielectric plate. The rod has a square cross section

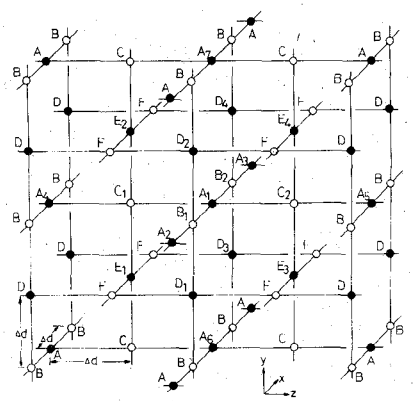

Fig. 2. Three-dimensional cubical lattice network.

(each side $20\Delta d$) and the length is $40\Delta d$. The aspect ratio is 2. The size of the land where the stripline and the rod are connected is a square of $40\Delta d$ on each side.

In this analysis we used a solid rod for simplicity of analysis as the fields propagate along the exterior surfaces. The relative dielectric constant is $\epsilon_r = 4.0$ for the substrate. The side faces of the substrate are terminated with the wave impedance $Z_0/\sqrt{\epsilon_r}$ (provided $Z_0 = 377$ Ω), which approximates the free boundary. For the input and output faces, load resistances are connected and adjusted so that they correspond to the characteristic impedances of the stripline. For clarity this is not shown in Fig. 1, but the domain actually analyzed included free spaces of depth $10\Delta d$ both above and below the structure in the y direction. The free boundary conditions for those regions also use the free-space impedance Z_0 in order to approximate the matching conditions. For the input conditions, we used a voltage with a sinusoidal wave of 20 GHz. The voltage was impressed at the node point between stripline a and the ground plate so that the electric field in the y direction, E_y, corresponded to the applied voltage through the characteristic impedance of the stripline.

B. Analysis Method

To explain the three-dimensional boundary conditions for the through hole of the previous section, we now describe the analysis method.

We represent and formulate the analyzed model by a three-dimensional network as shown in Fig. 2. Each branch of the network is a one-dimensional line. Lattice points are treated as node points. Each one-dimensional line has length equal to the separation distance Δd. We assume that, along each line, a TEM wave propagates with the Poynting vector along the line. The distribution of the fields is arranged to satisfy two-dimensional components of Maxwell's equations at node points which are the two terminals of each line. Voltages and currents are represented as circuit variables. Table I shows the equations for the relationship between the voltage and current and the field components of Maxwell's equations at each nodal point. Each letter for a node in the table corresponds to that node in Fig. 2. At each nodal point the

TABLE I

	Electric node			Magnetic node	
	Maxwell's Equ.	Variables		Maxwell's Equ.	Variables
A_k	$\frac{\partial H_x}{\partial z}-\frac{\partial H_z}{\partial x}=\varepsilon_0\frac{\partial E_y}{\partial t}$ $-\frac{\partial E_y}{\partial z}=-\mu_0\frac{\partial H_x}{\partial t}$ $\frac{\partial E_y}{\partial x}=-\mu_0\frac{\partial H_z}{\partial t}$	$V_y\equiv E_y$ $I_z\equiv -H_x$ $I_x\equiv H_z$	F_k	$\frac{\partial E_x}{\partial z}-\frac{\partial E_z}{\partial x}=-\mu_0\frac{\partial H_y}{\partial t}$ $-\frac{\partial H_y}{\partial z}=\varepsilon_0\frac{\partial E_x}{\partial t}$ $\frac{\partial H_y}{\partial x}=\varepsilon_0\frac{\partial E_z}{\partial t}$	$V_y^*\equiv H_y$ $I_z^*\equiv E_x$ $I_x^*\equiv -E_z$
D_k	$\frac{\partial H_z}{\partial y}-\frac{\partial H_y}{\partial z}=\varepsilon_0\frac{\partial E_x}{\partial t}$ $\frac{\partial E_x}{\partial z}=-\mu_0\frac{\partial H_y}{\partial t}$ $-\frac{\partial E_x}{\partial y}=-\mu_0\frac{\partial H_z}{\partial t}$	$V_x\equiv E_x$ $I_z\equiv H_y$ $I_y\equiv -H_z$	B_k	$\frac{\partial E_y}{\partial x}-\frac{\partial E_x}{\partial y}=-\mu_0\frac{\partial H_z}{\partial t}$ $\frac{\partial H_x}{\partial y}=\varepsilon_0\frac{\partial E_x}{\partial t}$ $-\frac{\partial H_z}{\partial x}=\varepsilon_0\frac{\partial E_y}{\partial t}$	$V_z^*\equiv H_z$ $I_y^*\equiv -E_x$ $I_x^*\equiv E_y$
E_k	$\frac{\partial H_y}{\partial x}-\frac{\partial H_x}{\partial y}=\varepsilon_0\frac{\partial E_z}{\partial t}$ $\frac{\partial E_z}{\partial y}=-\mu_0\frac{\partial H_x}{\partial t}$ $\frac{\partial E_z}{\partial x}=-\mu_0\frac{\partial H_y}{\partial t}$	$V_z\equiv -E_z$ $I_y\equiv -H_x$ $I_x\equiv H_y$	C_k	$\frac{\partial E_z}{\partial y}-\frac{\partial E_y}{\partial z}=-\mu_0\frac{\partial H_x}{\partial t}$ $\frac{\partial H_x}{\partial z}=\varepsilon_0\frac{\partial E_y}{\partial t}$ $-\frac{\partial H_x}{\partial y}=\varepsilon_0\frac{\partial E_z}{\partial t}$	$V_x^*\equiv -H_x$ $I_z^*\equiv E_y$ $I_y^*\equiv -E_z$
dielectric const. $C_0=\varepsilon_0/2$ permeability $L_0=\mu_0/2$				dielectric const. $L_0^*=\varepsilon_0/2$ permeability $C_0^*=\mu_0/2$	
polarization $\Delta C=\varepsilon_0\chi_e/2\cdot\Delta d$ conductivity $G=\sigma/2\cdot\Delta d$				magnetization $\Delta C_0^*=\mu_0\chi_m/2\cdot\Delta d$ magnetic current loss $G_0^*=\sigma^*/2\cdot\Delta d$	
magnetization $\Delta L=\mu_0\chi_m/2\cdot\Delta d$				polarization $\Delta L^*=\varepsilon_0\chi_e/2\cdot\Delta d$	

behavior is described for the fields in the plane which is perpendicular to the field components which represent voltage variables. They satisfy the two-dimensional Maxwell equations. The total basic lattice which includes all nodal points presents three-dimensional Maxwell's equations in discrete form by making the separation distance sufficiently small. In this method, a node where the voltage variable represents the electric field is called an electric node and is shown by a solid black circle in Fig. 2. A node where the magnetic field is represented by the voltage is called a magnetic node and is shown by an empty circle in Fig. 2. At magnetic nodes, the physical meanings of voltages and currents are opposite those adopted by the usual electric circuit theories. Table I distinguishes those variables with a superscript asterisk. The basic network is applied to the analyzed domain. The present method is suitable for the formulation of super-high-speed vector operations, which have been represented by supercomputers in the recent years. It has the feature of drastically reducing the calculation times.

C. Boundary Conditions of the Conductors

The equivalent circuit for the analyzed model of the fields includes the shapes of conductors, the free boundary conditions at the input and output terminal faces, and the conditions for the medium. In this section we describe the construction method for the equivalent circuit of the conductor surfaces, which provide the basic conditions for the conductor structure including a through hole.

As a basic condition, the conductor is assumed to have perfect conductivity. As a result, the tangential electric field is zero on the conductor surface. The magnetic field in the normal direction is zero. When we apply the present method to satisfy these conditions, we obtain the following two items as the boundary conditions at each nodal point.

i) The electric field in the tangential direction is represented at the node by either the voltage function or the current function, corresponding, respectively, to a shorted or an open terminal.
ii) The magnetic field in the normal direction is represented at the node by either the voltage function or the current function, corresponding, respectively, to a shorted or an open terminal.

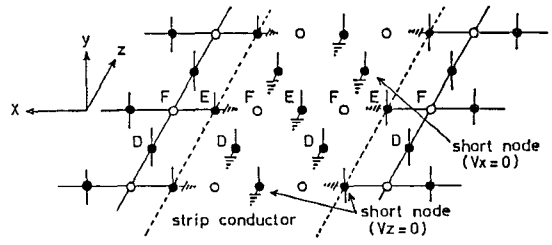

Fig. 3. Equivalent circuit of the surface of strip conductor.

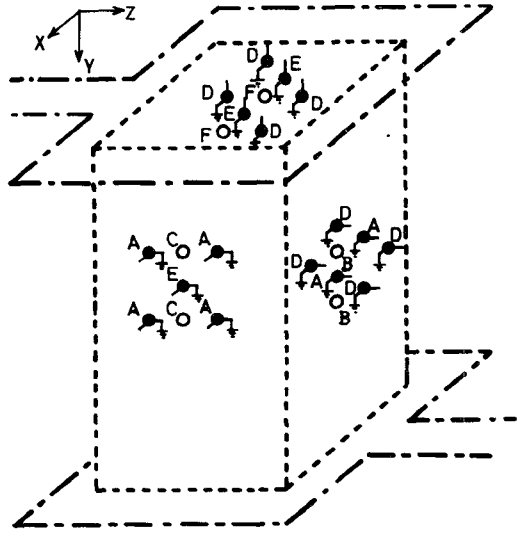

Fig. 4. Equivalent circuit of the rod conductor.

In the analyzed model we used the surfaces *DEF*, *ABD*, and *ACE* as conducting surfaces. When we apply the preceding boundary conditions, we obtain the equivalent circuits shown in Figs. 3 and 4. Fig. 3 is the equivalent circuit for the surfaces of the strip conductor and the ground plate. This $x-z$ plane is formed by node points *D*, *E*, and *F*. Now we explain the representation of the equivalent circuit. Based on Table I for voltages at nodes *D* and *E*, they correspond respectively to the tangential electric fields E_x and E_z on the conductor surface. By condition i) above, they are shorted. Fig. 3 shows grounding symbols for them. Consequently nodes *D* and *E* have no connection between upper and lower nodes. They are separated as points above or below the conductor. On the other hand, the voltage at node *F* corresponds to the normal magnetic field H_y. It is shorted according to condition ii) above. Currents in the x and y directions

correspond to tangential electric fields E_z and E_x, which are shown as open terminals by condition i). Every variable becomes zero and is shown isolated as in Fig. 3. Therefore its handling is easy, as there is no need for calculations. Fig. 4 is the equivalent circuit for the conductor surface of the rod conductor. Nodes A, B, and D form the $x-y$ plane, and nodes A, C, and E form the $y-z$ plane. As in the previous discussion for the $x-y$ plane, nodes A and D are shorted in the $x-y$ plane in Fig. 4 and node B is open and is also isolated. Based on Table I, the voltages at nodes A and E, respectively, become the tangential electric fields E_y and E_z on the $y-z$ plane. These components are zero and they are shorted.

D. Treatment of the Dielectric Material

The dielectric material is expressed as a capacitance and a conductance connected to the electrical node. As an example, Fig. 5 shows the equivalent circuit at A, at which the electric field E_y is a voltage function. The capacitance represents polarization and the conductance expresses conductivity. Since the analysis is based on the lossless assumption, the conductance is zero.

The equivalent circuit for the electromagnetic field for the model of Fig. 1 is constructed by including equivalent circuits for free boundary, terminal faces of input and output parts.

III. Derivation of the Far-Field Pattern from the Near Field

The method for calculating the far field in the present analysis is explained. In the present analysis, we use the surface component of the electric field on the $x-z$ plane that includes the upper land. When the field distributions on this surface are found, the far field can be given by using the following equation:

$$P_x(k_x,k_y)=\iint_S E_x(x,y)\exp\left[j(k_x x+k_y y)\right]dxdy \quad (1a)$$

$$P_y(k_x,k_y)=\iint_S E_y(x,y)\exp\left[j(k_x x+k_y y)\right]dxdy \quad (1b)$$

where E_x and E_y are the electric field components, k_x and k_y are the wavenumbers in the x and z directions, respectively, and S is the surface that contains the land. The far field is obtained by the following equation. Here, θ and ϕ are the angular variables in polar coordinates, k_0 is the free-space wavenumber, r is the distance from each point on surface, and i_ϕ and i_θ are the unit vectors in the ϕ and θ directions:

$$E_{(r)}=jk_0\frac{\exp(-jk_0r)}{2\pi r}\cdot\left\{\left[\left(P_y(\xi,\eta)\cos\phi-P_x(\xi,\eta)\sin\phi\right)\cos\theta\right]i_\phi+\left[P_x(\xi,\eta)\cos\phi+P_y(\xi,\eta)\sin\phi\right]i_\theta\right\} \quad (2)$$

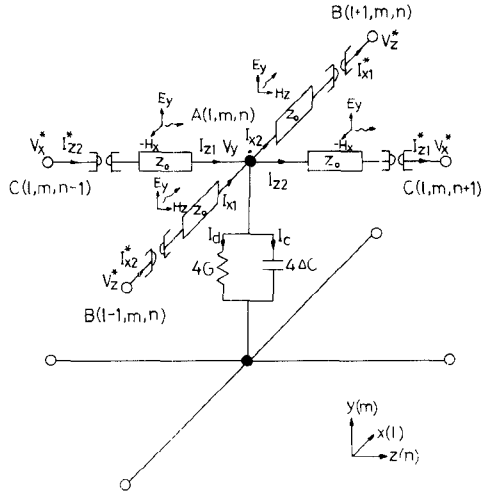

Fig. 5. Equivalent circuit of the node $A(l,m,n)$ with medium condition.

where

$$\xi=k_0\sin\theta\cos\phi$$
$$\eta=k_0\sin\theta\sin\phi.$$

The amplitude and phase of the electric field components in (1a) and (1b) are required. In the present time-domain analysis, they are found as follows. When sinusoidal waves are integrated from an arbitrary time point and the point is shifted by $\pi/2$ or $1/4$ period, sinusoidal and cosinusoidal functions are obtained which correspond to the imaginary and real parts of a complex quantity. At steady state, the electric field oscillates sinusoidally in time as follows:

$$E=E_0\sin(\omega t+\psi) \quad (3)$$

where E_0 is the amplitude, ω is the input angular frequency, t is time, and ψ is the reference phase. If the above is integrated from time t_0 for $T/4$ or $\pi/2$, where T is the period of the input wave,

$$E_1=\int_{t_0}^{t_0+T/4}E_0\sin(\omega t+\psi)\,dt=\sqrt{2}\,(T/2\pi)E_0\sin(\omega t_0+\psi+\pi/4). \quad (4)$$

Similarly, if the integration is for $T/4$ from $t+T/4$, then

$$E_2=\int_{t_0+T/4}^{t_0+T/2}E_0\sin(\omega t+\psi)\,dt=\sqrt{2}\,(T/2\pi)E_0\cos(\omega t_0+\psi+\pi/4). \quad (5)$$

Hence, if the complex representation of E is $\dot{E}$, then from (5) and (4),

$$\mathrm{Im}(\dot{E})=E_1(2\pi/T)/\sqrt{2} \quad (6)$$

$$\mathrm{Re}(\dot{E})=E_2(2\pi/T)/\sqrt{2}. \quad (7)$$

From (6) and (7), the amplitude and the phase can be derived. In actual numerical calculations, the time is discretized with a finite interval. Hence, if the number of discretizations of the period of the input wave is T_n, then the integration is over $T_n/4$ or $\pi/2$ (rad). If the results of the sum at each discretization time are E_1' and E_2', (6)

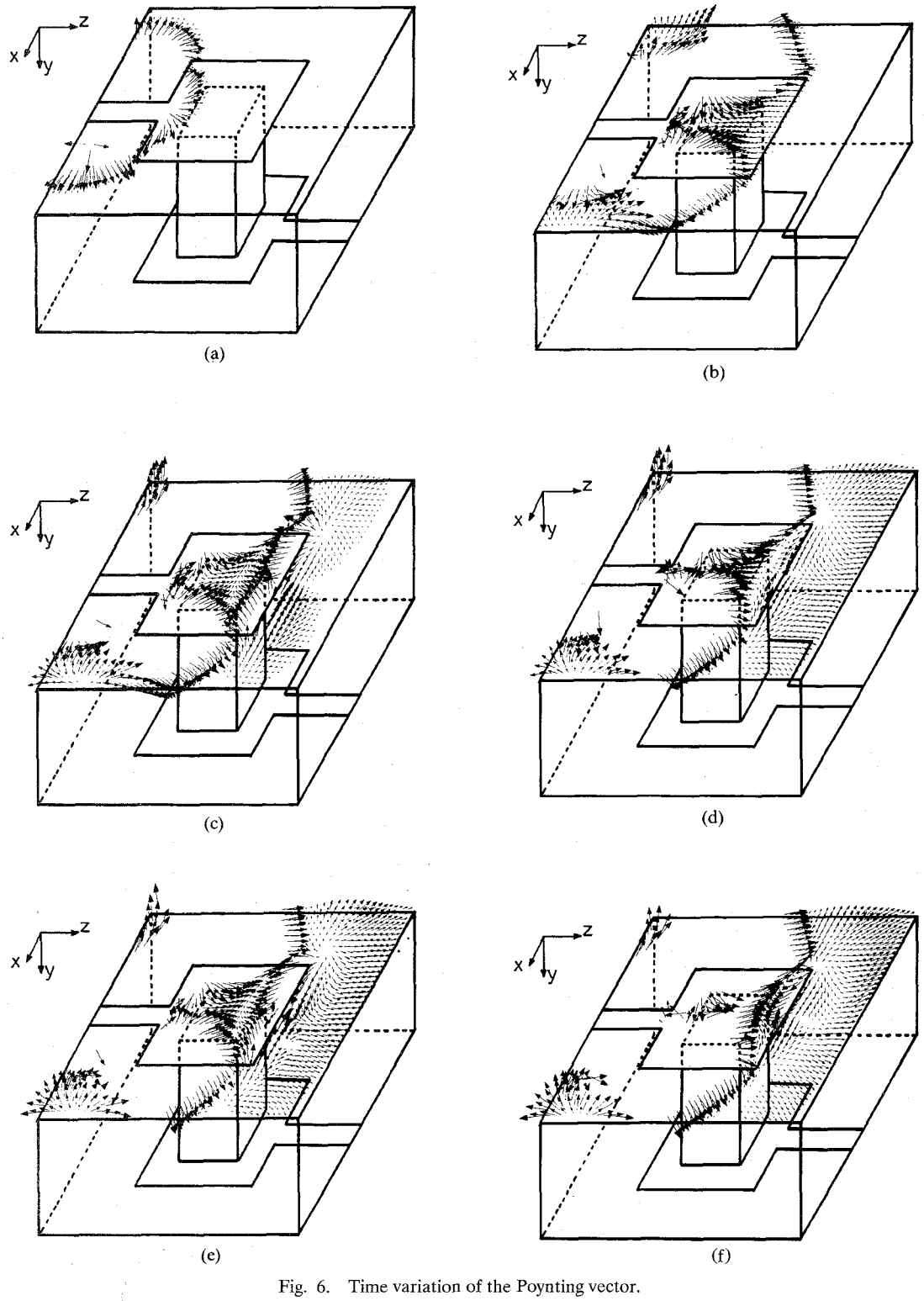

Fig. 6. Time variation of the Poynting vector.

and (7) become

$$\mathrm{Im}(\dot{E}) = E_1'(\pi/2)/(T_n/4)/\sqrt{2} \quad (8)$$

$$\mathrm{Re}(\dot{E}) = E_2'(\pi/2)/(T_n/4)/\sqrt{2}. \quad (9)$$

It is clear that the complex electric field is found by a simple addition on the time axis. This procedure is an algorithm suited for the spatial network method in time-domain analysis.

IV. Results of the Analysis

A. Time Response of the Spatial Distribution of the Poynting Vector

To observe the fundamental behavior of the energy flow near the through hole, we show the time response of the spatial distribution of the Poynting vector as an arrow mark (Fig. 6). The plane for observation is shown in Fig.

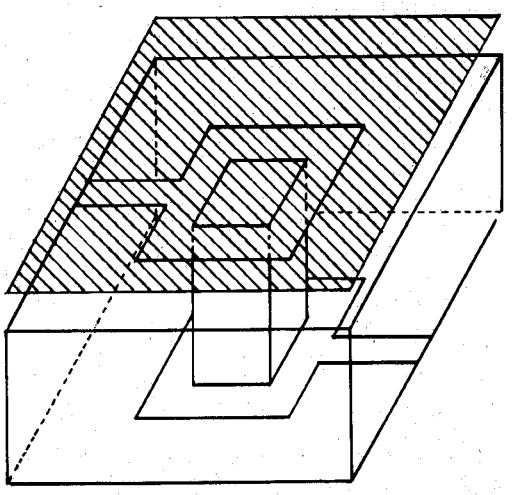

Fig. 7. Plane for observation.

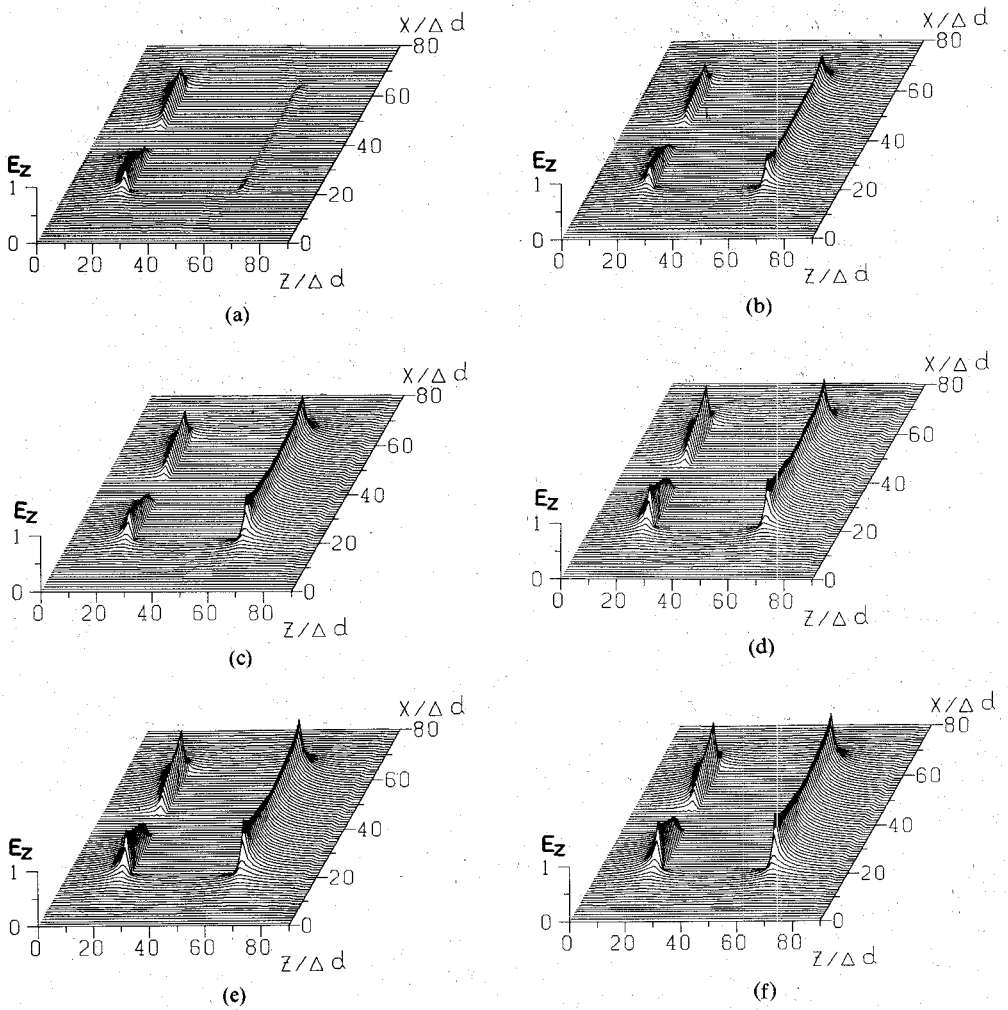

Fig. 8. Distribution of the electric field E_z in the plane including the land.

7. The length of the arrow corresponds to the magnitude, and the direction of the arrow shows that of the vector, respectively. In this analysis, the components of the vector which correspond to the radiation characteristics are required; thus the components of the vector to be expressed are limited to a very small magnitude. We drew the vectors whose magnitudes are less than 1/30 of the maximum value in every observation time. The observation time is every half-period of the wave. This interval corresponds 25 ps in real time. The observation plane of the Poynting vector is the $x-z$ plane $1\Delta d$ above the surface of the upper land. Near the edge of the stripline and the land, where the electric field is concentrated, the vectors are not drawn because they exceed the upper limit of the magnitude. And away from the strip and the land, the magnitude of the vectors seems to decrease rapidly.

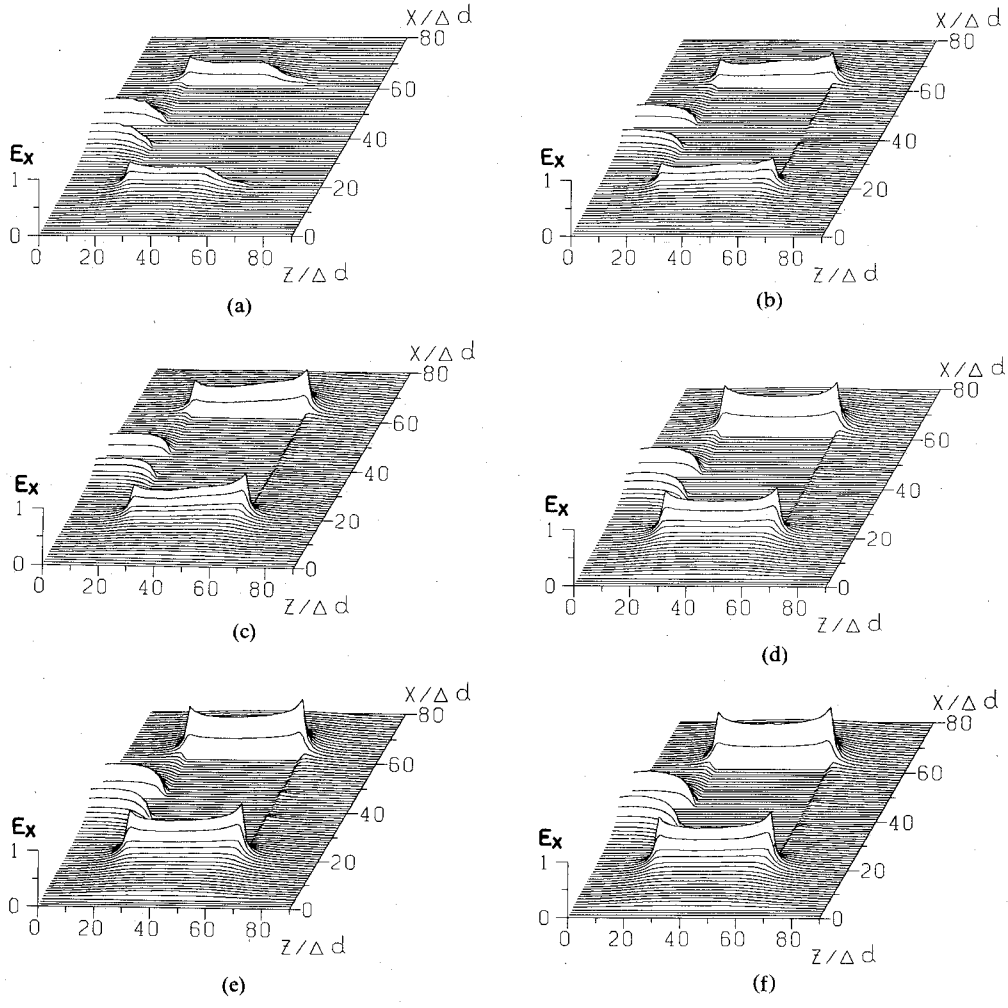

Fig. 9. Distribution of the electric field E_x in the plane including the land.

The direction of the vectors relatively far from the through hole is always outward since these vector components are supposed to correspond to radiation field components.

B. The Distribution of the Horizontal Electric Fields

Figs. 8 and 9 show the steady-state spatial distributions of the horizontal electric fields E_x and E_z in the upper land plane that mainly determines the far-field characteristics. The amplitude is normalized by the maximum value in each figure. In Fig. 8, E_z occurs almost along the edge in the x direction. The amplitude rapidly decays at a distance away from both edges and supposed to be the radiation sources as in the parallel slots model. In Fig. 9, E_x is shown to generate along the z-directed edge of the land and the strip. The amplitude of E_x is almost as large as that of E_z.

C. The Radiation Pattern

Lastly, the radiation patterns are computed from the spatial distributions of the electric field shown in Figs. 8 and 9, and the results are shown in Fig. 10(a) and (b) for the $x-y$ plane and in Fig. 10(c) for the $y-z$ plane. Fig. 10(a) is the pattern computed from the distributions of E_x and parts (b) and (c) of the figure are from that of E_z. Normalization is performed with the maximum value in these three figures. In this analysis the maximum value was that of Fig. 10(a). Due to the symmetry of the model in the x direction, the result in the $x-y$ plane also shows the symmetrical pattern. Though the land seems to have a structure similar to that of the path antennas, these results differ from those of the antennas because of the existence of the rod and the nonresonance frequency used.

V. Conclusions

We applied the spatial network method in analyzing a through hole to clarify the basic behavior of the field including radiation characteristics. The Poynting vector in the near field of the through hole, the distribution of the electric fields, and the far-field characteristics have been computed. From graphical representations of the Poynting vector near the land, the temporal and spatial properties of the energy flow corresponding to the radiation have been observed. The radiation patterns are calculated by adopting the Fourier transform in the near field of the electric fields obtained by the present method.

In this paper, the fundamental field distribution near the through hole and the basic properties of the radiation

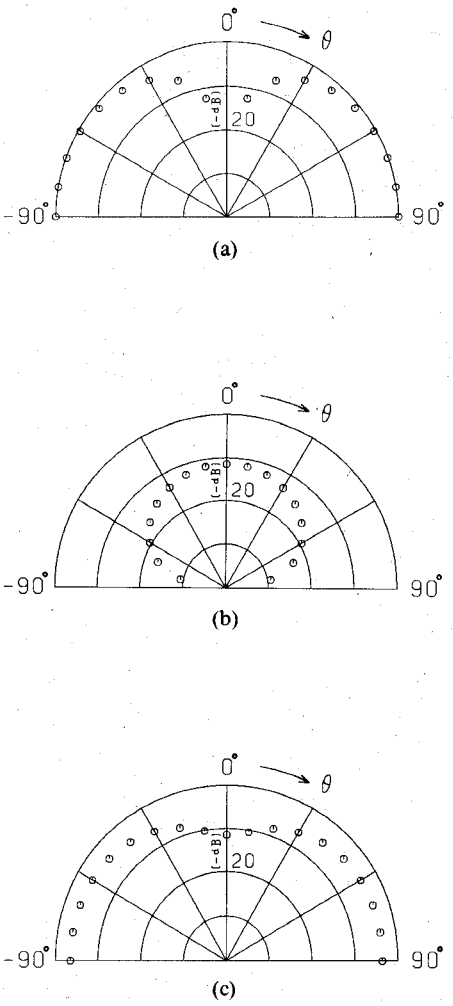

Fig. 10. (a) $x-y$ plane radiation pattern of E_x. (b) $x-y$ plane radiation pattern of E_z. (c) $y-z$ plane radiation pattern of E_z.

are described. The feasibility of applying the spatial network method to these problems is examined.

In a future paper the method will be applied to a more practical through hole model such as a circular one in a structure having more layers. Furthermore, unified analyses including other elements and devices will be needed to know and discuss the influences of a through hole on a total system.

References

[1] Editors for Electronic Materials, "Technology of printed circuit plates," Industrial Examination Committee, Tokyo, (1985).

[2] N. Yoshida, I. Fukai, and J. Fukuoka, "Analysis of transient solution by nodal equations of electromagnetic fields," *Trans. IEC Japan(B)*, vol. J63-B, pp. 876–883, Sept. 1980.

[3] N. Yoshida and I. Fukai, "Transient analysis of a stripline having a corner in three-dimensional space," *IEEE Trans. Microwave Theory Tech.*, vol. MTT-32, pp. 491–498, May 1984.

[4] E. Yamashita, "Fundamental analysis method for problems of electromagnetic wave," Ch. 5, pp. 130–164, *IEICE Japan Tokyo*, 1987.

[5] S. Koike, N. Yoshida, and I. Fukai, "Transient analysis of microstrip gap in three-dimensional space," *IEEE Trans. Microwave Theory Tech.*, vol. MTT-33, pp. 726–730, Aug. 1985.

[6] S. Koike, N. Yoshida, and I. Fukai, "Transient analysis of a directional coupler using a coupled microstrip slot line in three-dimensional space," *IEEE Trans. Microwave Theory Tech.*, vol. MTT-34, pp. 353–357, Mar. 1986.

[7] S. Koike, N. Yoshida, and I. Fukai, "Transient analysis of coupling between crossing-lines in three-dimensional space," *IEEE Trans. Microwave Theory Tech.*, vol. MTT-34, pp. 67–71, Jan. 1987.

[8] N. Masuzuka, S. Koike, N. Yoshida, and I. Fukai, "Transient analysis of three-dimensional electromagnetic field in through-hole," *Trans. IEICE Japan*, vol. E70, pp. 703–705, Aug. 1987.

[9] N. Masuzuka, N. Yoshida, and I. Fukai, "A three-dimensional analysis of the electromagnetic fields of a through-hole," *Trans. Microwave, IEICE Japan*, vol. MW-87-39, July 1987.

[10] N. Masuzuka, N. Yoshida, and I. Fukai, "Three-dimensional field analysis of a through-hole," *Trans. Electron. Circuits, IEE Japan*, vol. ECT-87-15, Sept. 1987.

[11] N. Masuzuka, N. Yoshida, and I. Fukai, "Transient analysis of three-dimensional electromagnetic field in through-hole," *Trans. IEICE Japan(C)*, vol. J71-C, 7, pp. 986–993, July 1988.

[12] T. Kashiwa, S. Koike, N. Yoshida, and I. Fukai, "Three-dimensional analysis of patch antenna by Bergeron's method," *Trans. IEICE Japan(B)*, vol. J71-B, pp. 576–584, Apr. 1988.

[13] T. Onojima, T. Kashiwa, N. Yoshida, and I. Fukai, "Analysis of radiation characteristics from a through-hole in the multilayer print board," *Trans. Electronmagn. Theory, IEE Japan*, vol. EMT-89-43, May 1989.

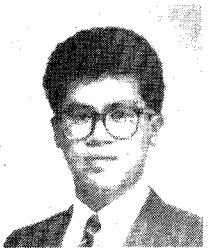

Tohru Onojima was born in Hokkaido, Japan, on August 16, 1964. He received the B.E. degree in electrical engineering from Hokkaido University, Sapporo, Japan, in 1988. He is presently working towards the M.E. degree in electrical engineering at the same university. He is now interested in the transient analysis of through holes in three-dimensional space.

Mr. Onojima is an associate member of the Institute of Electronics, Information and Communication Engineers in Japan.

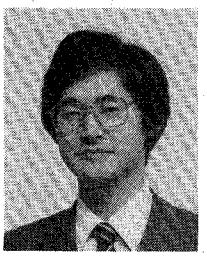

Tatsuya Kashiwa (M'88) was born in Hokkaido, Japan, on June 3, 1961. He received the B.E. and M.E. degrees in electrical engineering from Hokkaido University, Sapporo, Japan, in 1984 and 1986, respectively.

He became a research assistant in the same university in 1988. His current research interests center on the transient analysis of plasmas and antennas in three-dimensional space.

Mr. Kashiwa is a member of the Institute of Electronics, Information and Communication Engineers in Japan.

Norinobu Yoshida (M'87) was born in Hokkaido, Japan, on May 27, 1942. He received the B.E. and M.E. degrees in electronics engineering from Hokkaido University, Sapporo, Japan, in 1965 and 1967, respec-

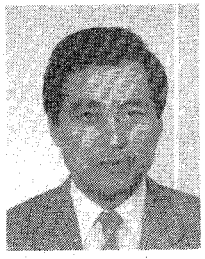

tively, and the D.E. degree in electrical engineering from the same university in 1982.

He joined the Nippon Electric Company, Ltd., Tokyo, in 1967, where he worked in computer-aided design in the Integrated Circuit Division. He became a Research Assistant in 1969 in the Department of Electrical Engineering in the Faculty of Engineering of Hokkaido University. He became a Lecturer there in 1983 and an Associate Professor in 1984 in the same department. He is presently engaged in research on numerical methods for the transient analysis of electromagnetic fields.

Dr. Yoshida is a member of the Institute of Electrical Engineers of Japan and the Institute of Electronics, Information and Communication Engineers in Japan.

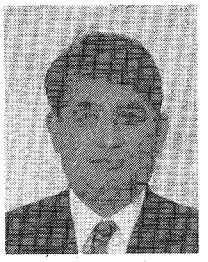

Ichiro Fukai (M'87) was born in Hokkaido, Japan, on August 21, 1930. He received the B.E., M.E., and D.E. degrees in electrical engineering from Hokkaido University, Sapporo, Japan, in 1953, 1956, and 1976, respectively.

In 1956, he joined the Defense Agency Technical Research and Development Institute. He became a Research Assistant in 1959 in the Faculty of Engineering of Hokkaido University and an Associate Professor at the Technical Teacher's Training Institute in 1961. In 1968 he became an Associate Professor and in 1977 a Professor in the Department of Electrical Engineering of the Faculty of Engineering at Hokkaido University.

Dr. Fukai is a member of the Institute of Electrical Engineers of Japan and the Institute of Electronics, Information and Communication Engineers in Japan.